Understanding H-defect complexes in ZnO

R. Vidya[1,2],* P. Ravindran[1,3], and H. Fjellvåg[1]
[1] *Center for Materials Science and Nanotechnology and Department of Chemistry, University of Oslo, Box 1033 Blindern, N-0315 Oslo, Norway*
[2] *Institute of Mathematical Sciences, CIT Campus, Taramani, Chennai 600 113, India and*
[3] *Department of Physics, Central University of Tamil Nadu, Thiruvarur, Tamil Nadu, 610 001, India*
(Dated: September 20, 2013)

From state-of-the-art density-functional calculations using hybrid functionals we show that, persistent n-type conductivity in ZnO is due to defect complexes formed between H with intrinsic and extrinsic defects. H exhibits cationic, anionic, and electrically-inactive character on interacting with defects in ZnO. The electrically-inactive molecular hydrogen can contribute to n-type conductivity in ZnO by activating deep donor levels into shallow levels. By calculating local vibrational mode frequencies, we have identified origins of many H-related Raman and infra-red frequencies and thus confirmed the amphoteric behavior of H.

PACS numbers: 71., 81.05.Je, 71.15.Nc, 71.20.-b, 81.40.Rs

ZnO is one of the the most studied wide band-gap (E_g) semiconductors because of its wide range of applications. Though as-prepared samples of ZnO contain many impurities, interaction of ubiquitous impurity like H with ZnO has many important technological implications. For example, H is expected to become an environmentally-benign fuel in future and nanophase ZnO can be a potential sensor for H because of its excellent characteristics [1]. Moreover, ZnO is considered as a prospective material for hydrogen storage in future [3] because high amount of hydrogen (30.5 at.%) can be introduced into ZnO crystals by electrochemical charging. The stability of ZnO against hydrogen plasma makes it interesting also for solar cell applications where ZnO is used as a transparent-conducting electrode [2]. Therefore it is vital to understand the influence of H on properties of ZnO.

ZnO exhibits n-type conductivity even without deliberate doping. Introduction of hydrogen into ZnO at elevated temperatures was shown to give rise to the n-type conductivity [4, 5]. First-principles investigations [6, 7] substantiated that interstitial H (H_i) and substitutional H (H_O) are indeed shallow donors and contribute to the n-type conductivity. By annealing hydrogenated ZnO samples, 78% of the free carriers were eliminated near 150^oC and the remainder between $500-700^oC$ [8]. However H_i is shown [9, 10] to be unstable above room temperature, making it difficult to understand how hydrogen alone can give rise to conductivity at high temperatures. Moreover, the donor levels from H_i and H_O are shown to be resonant inside conduction band whereas various experimental techniques [5, 10–16], observed a H-related shallow donor level at $25-50$ meV below conduction band minimum (CBM) whose origin is not clearly understood.

In addition, many vibrational frequencies have been measured in ZnO by infra-red (IR) spectroscopy whose origins are still puzzling. For example, the prominent peak at 3326 was earlier believed to be related to H_i at anti-bonding ($AB_{O,\perp}$) [8] and later assigned to V_{Zn}+H_i [17] and Ca_{Zn}+H_i complex [18]. The peak at 3611 cm^{-1} is assigned to H_i at bond-centered ($BC_{\parallel}$) site [15], but impurity-hydrogen complex was not ruled out as this peak was stable up to 350^oC in annealing experiments [31]. IR and Raman spectroscopy can provide valuable clues about the nature of a defect, from frequency and symmetry of the observed modes. However, comparison of these values with first-principles calculations can provide a conclusive microscopic identification of a defect [20].

We have performed first-principles calculations using the projected augmented plane-wave method [21] implemented in the Vienna *ab initio* simulation package (VASP) [22]. Complete structural optimizations with H at various interstitial/substitutional positions, without and with impurities like Li, B, C, N, Al, and Ga in different charge states were done. Supercells of 192 atoms with a plane-wave energy cutoff of 550 eV were used. The atomic geometry was optimized by force as well as stress minimizations with convergence criteria of 10^{-6} eV per unit cell for total energy and ≤ 1 meV $Å^{-1}$ for forces. Exchange and correlation effects are treated under the generalized-gradient-approximation [23] with Perdew-Burke-Ehrenkof functional. To identify the origin of experimentally-observed IR and Raman-active phonon mode frequencies, we have derived the local vibrational mode (LVM) frequencies from "frozen-phonon" calculations. The concerned atoms are displaced in steps of 0.001 Å to a maximum of 0.005 Å in both directions to account for possible anharmonic effects. More details are given in Ref. 27 where the calculated frequencies are shown to be within 10 cm^{-1} from experimental values.

Finally one set of structure optimization and electronic structure calculation was carried out using the Heyd-Scuseria-Ernzerhof (HSE) hybrid functional [24] with a screening parameter of $a = 0.375$ which reproduced the experimental structural parameters and band-gap value for ZnO. The total energy obtained using HSE functional

*Electronic address: vidya.ravindran@smn.uio.no

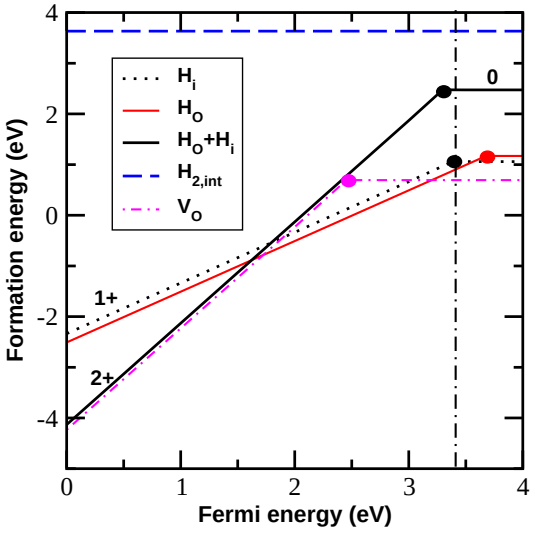

FIG. 1: (Color online) Formation energy of defects obtained using hybrid functionals (under Zn-rich conditions). The dots indicate charge-transition points and the charge states are given on the illustration.

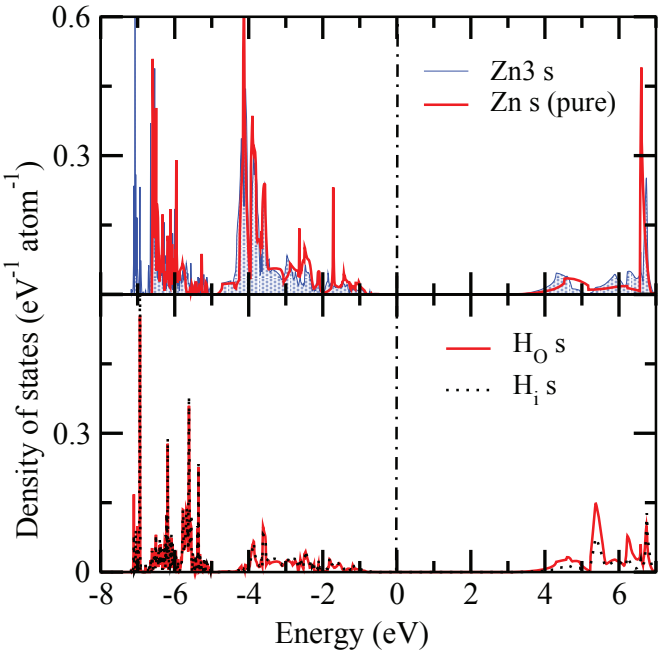

FIG. 2: (Color online) Density of state for s-orbitals of H in the H_O+H_i complex and s-orbitals of the neighboring Zn atoms that is displaced along z-axis (see text). For comparison, Zn-s orbitals in pure ZnO is shown in red (solid) lines.

is used to derive defect formation energy and thermodynamic transition levels of various defects as described in Refs. 25, 26.

Hydrogen is shown to be commonly present in as-grown ZnO samples. Diffusion of H_i due to annealing of sample at 150^{o}C [8] was suggested to form interstitial H_2 molecule which is "hidden" from experimental techniques like IR, ESR measurements etc. The Raman frequency for this so-called "hidden" hydrogen is recently measured to be 4145 cm^{-1} [15]. In order to understand formation of "hidden" hydrogen better, we modeled H at six different interstitial positions (H_i), H at oxygen vacancy (H_O), and H_2 molecule in the interstitial channel ($H_{2,int}$) oriented along x, y, z directions. We found that $H_{2,int}$ along z-direction in neutral state has the lowest formation energy among its counterparts oriented along x and y directions. However, the formation energy of H_i and H_O is lower compared to that of $H_{2,int}$. The calculated Raman frequency for $H_{2,int}$ along z-direction is 4047 cm^{-1}, in agreement with previous theoretical study [9]. It can be seen from Fig. 1 that $H_{2,int}$ has the highest formation energy among other H-related defects considered.

It has been well established that the oxygen vacancy (V_O) is the dominant intrinsic defect in ZnO [6, 25]. When V_O is formed, electrons from dangling bonds of surrounding Zn sites are localized at the vacancy [26]. We have shown [28] that H prefers to occupy sites where non-bonding localized electron density is maximum and where it could obtain maximum screening [7]. In conjunction, when H occupies the V_O (H_O), the surrounding Zn atoms are relaxed towards H_O. As V_O prefers to be in 2+ state, we introduced another interstitial H close to H_O, and thus modelled two configurations: (i) H_O and a H_i at $BC_\parallel$ and (ii) H_O and a H_i at $AB_{O,\perp}$ (see Fig. 3c). Interestingly, the H_i placed at a distance of 0.98 Å from H_O, relaxes towards H_O and forms a complex with a H_O-H_i distance of 0.76 Å. It is worthwhile to note that the H−H distance in gaseous H_2 is 0.74 Å. Hence the H_O+H_i complex can be visualized as a H_2 molecule trapped at a V_O. Formation energy of this complex is nearly 1.25 eV lower than the isolated $H_{2,int}$ molecule (Fig. 1).

Interestingly, the calculated Raman frequencies for H_O+H_i($BC_\parallel$) and H_O+H_i($AB_{O,\perp}$) are 4103 and 4108 cm^{-1}, respectively, in better agreement with experimental value than that for $H_{2,int}$ (see Table 1). The calculated Raman frequency for D_O+D_i complex (2908 cm^{-1}) is also in good agreement with experimental value of 2985 cm^{-1}. Thus, H_O+H_i complex could be a better candidate for the so-called "hidden" hydrogen in ZnO, in line with the recent calculations [29].

In addition to the 4145 cm^{-1} line, a weaker component blue-shifted by 8 cm^{-1} was also observed [15], believed to be due to the ortho-para splitting of the interstitial H_2 molecule in ZnO. The calculated formation energy of H_O+H_i($BC_\parallel$) is only slightly higher (2 meV) than H_O+H_i($AB_{O,\perp}$). Therefore H_i in the H_O+H_i complex can easily move from the $AB_{O,\perp}$ site to the $BC_\parallel$ site, leading to a difference in Raman frequency of 5 cm^{-1}. Hence, in addition to the ortho-para splitting of the H_2 molecule (trapped at V_O), different geometric orientations of the H_O+H_i complex could also lead to the observed blue-shift of the Raman frequency.

The H_O+H_i complex has the lowest formation energy (up to mid-gap value; Fig. 1) among H-related defects

considered. While the 1+ to 0 transition of H_i occurs exactly at CBM, the H_O has the same at 0.3 eV above the CBM. On the other hand, the H_O+H_i complex is stable in 2+ state for most of the Fermi energy values and the 2+ to 0 transition occurs at 50 meV below CBM (shallow donor level). This could explain the electrical conductivity measurements (40−51 meV) made in 1950s [5, 11] and the following experimental observations: The ionization energy of H in ZnO is 35±5 meV by EPR measurements [10, 12]. The Hall measurements on vapor-phase grown samples showed a H donor level at 30-40 meV which increased to 50 meV upon increasing temperature. Hydrogen-implanted hydrothermal-grown ZnO films and ZnO annealed in Zn-rich (O-deficient) conditions also showed a donor level ≈ 45 meV that was stable at high temperatures [14, 16]. The photoluminescence spectra exhibit a sharp excitonic feature at 3.363 eV (known as I_4 line; optical fingerprint of H in vapor-phase grown ZnO [13]) very close to where we observe the 2+ to 0 transition of the H_O+H_i complex.

Usually H_2 is believed to be electrically inactive, whereas the present study shows that a shallow donor level is created when H_2 occupies V_O. To understand the mechanism leading to the formation of this shallow level we analyzed the electronic structure in detail. The calculated DOS using HSE functional ($E_g = 3.3$ eV) show that s-orbitals of H_O and H_i are well-localized with sharp peaks between −8 to −6 eV, implying that the H_O+H_i complex is electrically-inactive. The charge density surrounding the H_O+H_i complex clearly substantiates its molecular-like character (Fig. 3a).

To obtain more insight, the DOS of Zn atoms surrounding the H_O+H_i complex is compared with that of pure ZnO (shaded DOS in Fig. 2). The Zn-p and Zn-d states of Zn atoms surrounding the complex are not changed very much compared to those in pure ZnO. However, the unoccupied Zn-s levels are shifted to lower energy from CBM. When H_2 occupies the V_O, the surrounding Zn atoms are relaxed outwards from V_O. The bond-lengths of Zn1, Zn2, and Zn4 with their neighbors increase by nearly 24.5% compared to that in pure ZnO. Zn3 moves away along z-axis by 28.3% to compensate the repulsive interaction from electrons at the H_O+H_i complex. Therefore Zn3 occupies an interstitial site and becomes co-planar with the neighboring O atoms. The charge density clearly shows an overlap interaction of Zn-s states with O-s states along z direction (see arrow in Fig. 3a) as a result of the displacement of the Zn3 atom. In agreement with the above inference, the muon-electron contact hyperfine interaction showed [30] a shallow level at 60 ± 10 meV below CBM with a highly dilated electron wave function of Zn-4s character. Thus the electrically-inactive H_2 molecule at V_O indirectly introduces an overlap interaction between neighboring Zn and O, which activates the deep donor level from V_O^{2+} into a shallow level (Fig. 1).

Our nudged-elastic band (NEB) calculations show that the H_O+H_i complex is 0.38 eV higher in energy than isolated H_O and H_i. Moreover, the reaction barrier to form the H_O+H_i complex from isolated H_O and H_i is 0.92 eV indicating that it can be formed at high temperatures. The migration barrier for a $H_{2,int}$ to occupy a V_O is calculated to be less than 19 meV, indicating that molecular H prefers to occupy the V_O than to be at the interstitial channel. As V_O is formed at elevated temperature, H_2 molecule can occupy the V_O to form the H_O+H_i complex, consistent with experimental observation [8]. It may be noted that the experimentally established [4, 5] activation energy of a H-related donor at 40 meV observed at high temperature is 0.91−1.12 eV, in good agreement with our finding. This implies that the H_O+H_i complex could be a meta-stable species and could explain the conductivity measurements on ZnO at high temperatures.

TABLE I: Local vibrational mode frequencies (in cm^{-1}) of hydrogen in ZnO. The identified origin of the frequencies, the corresponding H positions and orientations are given.

Frequency		Origin	H position	Orientation
Expt. [Ref.]	Present			
4145 [15]	4108	H_O+H_i	$AB_{O,\perp}$	–
-	4047	$H_{2,int}$	∥c	–
-	338		H_O+H_i	$BC_\parallel$ –
-	560	Li_{Zn}+H_O	V_O	∥c
3611 [31]	3621	B_{Zn}+H_i	$BC_\parallel$	∥c
3326 [32]	3337	Al_{Zn}+H_i	$AB_{O,\perp}$	⊥c
3349 [31]	3339	V_{Zn}+2H_i	$AB_{O,\perp}$	⊥c
-	3352	Ga_{Zn}+H_i	$BC_\parallel$	∥c
3312 [31]	3312	Al_{Zn}+H_i	$BC_\parallel$	∥c

Many H-related vibrational frequencies have been measured in ZnO by IR spectroscopy, in particular absorption peaks at 3611 and 3326 cm^{-1} are the most prominent frequencies. As ZnO can be prepared by many different synthetic techniques and conditions, incorporation of different impurities becomes unavoidable. Although frequency and symmetry of the observed modes from IR and Raman spectroscopy can provide valuable clues about the nature of a defect, comparisons with first-principles calculations are needed to provide a conclusive microscopic identification of a defect [20]. In order to isolate the role of individual defects, we have calculated energetics and IR frequencies of H in different interstitial positions as well as with company of other impurities.

The calculated LVM of H at various interstitial/substitutional positions together with other defects/impurities are given in Table I. The calculated LVM for isolated H_i at $BC_\parallel$, $AB_\parallel$, $BC_\perp$, and $AB_\perp$ are 3565, 3440, 2540, and 3155 cm^{-1}, respectively. On the other hand, the calculated LVM for H_i at $BC_\parallel$ adjacent to B_{Zn} (Boron at V_{Zn}; Fig. 3b) gives a value of 3621 cm^{-1}, in excellent agreement with experiment. Interestingly, the samples grown by CVD have Boron as one of the dominant impurities which lead to the peak at 3611 cm^{-1} [34]. Moreover, for H_i at $AB_\perp$ adjacent to Al_{Zn} the calculated frequency is 3337 cm^{-1}, in good agreement with

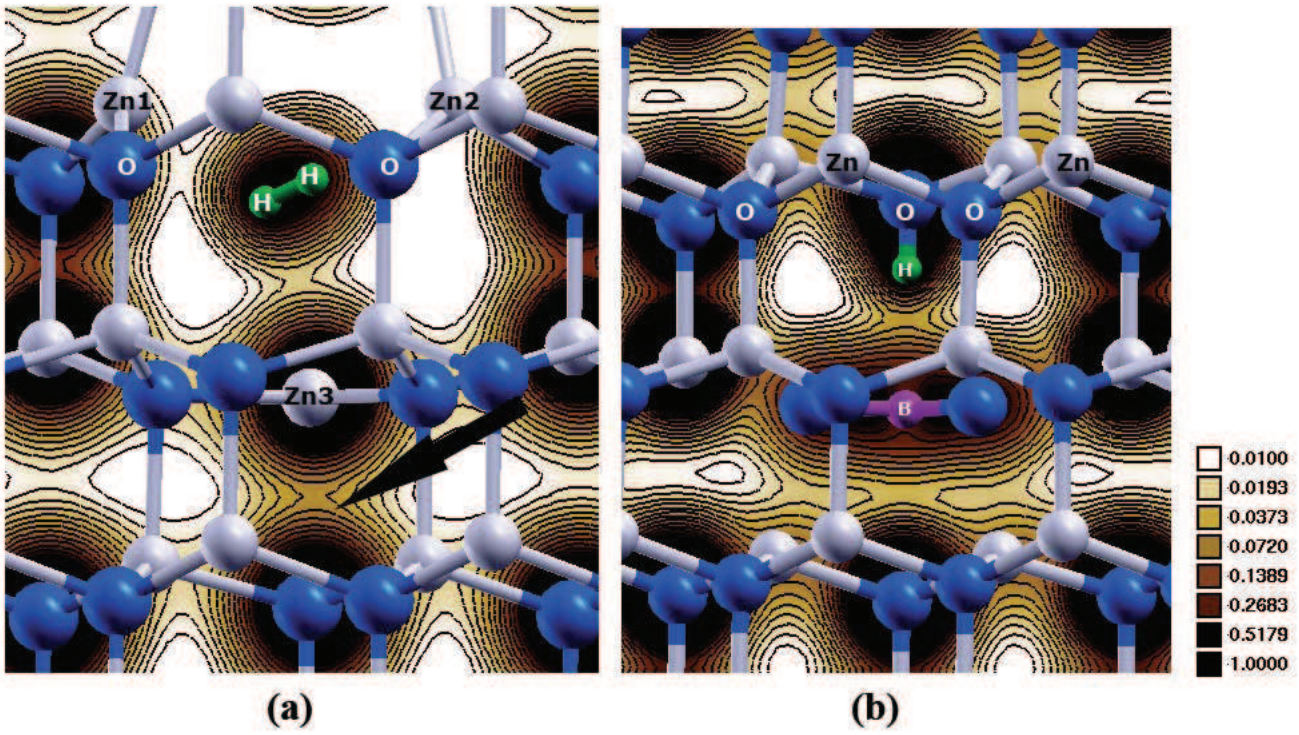

FIG. 3: (Color online) Electronic charge density of ZnO showing (a) electrically neutral H_O+H_i; Bonding states arising due to Zn displacement are shown by arrow (b) cationic H in B_{Zn}+H_i at $BC_{\parallel}$.

experimental value. It is noteworthy that SIMS measurements [34] showed significant concentrations of Al in the melt-grown samples that have the dominant peak at 3326 cm^{-1} [35]. The experimental frequencies are dependent on sample preparation and annealing conditions [20, 33], substantiating our findings that the observed hydrogen modes could also arise from impurity-hydrogen complexes. Interestingly, these complexes are stable in 2+ charge state, implying their contribution to the n-type conductivity in ZnO where H has a cationic character. Even though we have considered as many impurity+H complexes as possible within computational limitations, other defect complexes leading to the observed frequencies can not be completely ruled out.

As seen above, H by attaching to O exhibits cationic character with impurities like B, and Al (Fig. 3b) like in the case of proton-conducting oxides. Additional calculations show that anionic H (H_O close to Li_{Zn}) is energetically more favorable than cationic H in the company of Li_{Zn}. When H occupies an intrinsic defect like V_O, it takes up anionic character (as in ionic hydrides) and brings in n-type conductivity at ambient conditions. In contrast, in molecular H and organic solids, H is neutral and forms strong covalent bonding. As shown in Fig. 1 and Fig. 3a, this neutral H_2 at V_O induces shallow donor level at high temperatures in ZnO. The frequencies 3611 and 4145 cm^{-1} are measured in the same sample under different annealing conditions [15, 36]. Our calculations show that formation of cationic H (H_i close to B_{Zn} and Al_{Zn}), neutral (H_2 at V_O) and, anionic H (H_O close to Li_{Zn}) is energetically favorable and lead to the often-observed IR and Raman frequencies in ZnO. This implies that H can exhibit amphoteric behavior in the same sample under different conditions. This chemically-adaptable versatile nature of H makes it stable with the company of both donor and acceptor-type impurities. However, H always induces n-type conductivity with intrinsic and extrinsic defects in spite of its amphoteric behavior as shown above. This could explain the persistent n-type conductivity of ZnO at low as well as high temperatures.

In this letter we have shown that even the electrically-inactive molecular hydrogen is shown to activate deep donor levels and thus bring in n-type conductivity. H can exhibit cationic, anionic and neutral character in a single material under different conditions. The defect complexes formed between H and prominent impurities like Li, B, and Al could give rise to the H-related local vibrational modes in ZnO and enhance its n-type conductivity. Therefore these impurities should be removed by annealing treatments to bring in p-type conductivity in ZnO. We have demonstrated that experimental results together with present type of theoretical calculations are needed to characterize impurities in semiconductors unambiguously.

The authors are grateful to the Research Council of Norway for financial support (DESEMAT project under FRIENERGI program) and computing time on the Norwegian supercomputer facilities (NOTUR). RV thanks

Institute of Mathematical Sciences for hospitality.

[1] Y.J. Chen, et.al., Appl. Phys. Lett. **87**, 233503 (2005).
[2] W. Beyer, J. Hupkes, and H. Stiebig, Thin Solid Films **516**, 147 (2007).
[3] J. Čížek, et.al., J. Appl. Phys. **103**, 053508 (2008).
[4] E. Mollwo, Z. Physik, **138** 478 (1954).
[5] D.G. Thomas and J.J. Lander, J. Chem. Phys. **25**, 1136 (1956).
[6] C.G. Van de Walle, Phys. Rev. Lett. **85**, 1012 (2000).
[7] A. Janotti and C.G. Van de Walle, Nature Mater. **6**, 44 (2007).
[8] G. A. Shi, M. Saboktakin, M. Stavola, and S.J. Pearton, Appl. Phys. Lett. **85**, 5601 (2004).
[9] M.G. Wardle, J.P. Goss, and P.R. Briddon, Phys. Rev. Lett. **96**, 205504 (2006).
[10] K. Ip, M. E. Overberg, et.al., Appl. Phys. Lett. **82**, 385 (2003).
[11] A. R. Hutson, Phys. Rev. **108**, 222 (1957).
[12] D.M.Hofmann, A. Hofstaetter, et.al., Phys. Rev. Lett. 88, 045504 (2002).
[13] D.C. Look, et.al., Physica B **340-342**, 32 (2003).
[14] G. H. Kassier, et.al., Phys. Stat. Sol. (c) **5**, 569 (2008).
[15] E. V. Lavrov, F. Herklotz, and J. Weber, Phys. Rev. Lett. **102**, 185502 (2009).
[16] M.H. Weber, et.al., J. Electronic Mat. **39**, 573 (2010).
[17] F. Herklotz, E.V. Lavrov et.al. Phys. Rev. B bf 82, 115206 (2010).
[18] X.-B. Li, S. Limpijumnong, et.al., Phys. Rev. B **78**, 113203 (2008).
[19] E. V. Lavrov, F. Börrnert, and J. Weber, Phys. Rev. B **72**, 085212 (2005).
[20] C.G. Van de Walle and J. Neugebauer, Annu. Rev. Mater. Res. **36**, 179 (2006).
[21] P. E. Blöchl, Phys. Rev. B **50**, 17953 (1994).
[22] G. Kresse and J. Fürthmuller, Comput. Mater. Sci. **6**, 15 (1996).
[23] J.P. Perdew, K. Burke, and M. Ernzerhof, Phys. Rev. Lett. **77**, 3865 (1996).
[24] J. Heyd, G. E. Scuseria, and M. Ernzerhof, J. Chem. Phys. **118**, 8207 (2003); **124**, 219906 (2006).
[25] F. Oba, A. Togo, et.al., Phys. Rev. B **77**, 245202 (2008).
[26] R. Vidya, P. Ravindran, H. Fjellvåg, et.al., Phys. Rev. B **83**, 045206 (2011).
[27] P. Ravindran, A. Kjekshus, H. Fjellvåg, et.al., Phys. Rev. B 67, 104507 (2003).
[28] P. Vajeeston, P. Ravindran, et.al., Euro. Phys. Lett. **72**, 569 (2005).
[29] M.-H. Du and K. Biswas, Phys. Rev. Lett. **106**, 115502 (2011).
[30] S.F.J. Cox, E.A. Davis, et.al., Phys. Rev. Lett. **86**, 2601 (2001).
[31] E. V. Lavrov, J. Weber, et.al., Phys. Rev. B **66**, 165205 (2002).
[32] M.D. McCluskey, et.al., Appl. Phys. Lett. **81**, 3807 (2002).
[33] S.J. Jokela and M.D. McCluskey, Phys. Rev. B **76**, 193201 (2007).
[34] M.D. McCluskey and S.J. Jokela, Physica B **401-402**, 355 (2007).
[35] S.J. Jokela, M.D. McCluskey, and K.G. Lynn, Physica B **340-342**, 221 (2003).
[36] E.V. Lavrov, Physica B **404**, 5075 (2009).
[37] E.V. Lavrov, Physica B **340-342**, 195 (2003).
[38] M. G. Wardle, J. P. Goss, and P. R. Briddon, Phys. Rev. B **71**, 155205 (2005).